Brain Inspired Cognitive Systems
August 29 – September 1, 2004
University of Stirling, Scotland, UK

CREATION OF A CUSTOM BASIS FOR DETECTION OF A NEURAL PHYSIOLOGICAL EVENT IN EEG

Philip M. Zeman, University of Victoria Assistive Technology Team, University of Victoria, BC, CANADA

Nigel Livingston, University of Victoria Assistive Technology Team, University of Victoria, BC, CANADA
W. H. Hook, Department of Forest Biology, University of Victoria, BC, CANADA
Peter F. Driessen, Department of Engineering, University of Victoria, BC, CANADA

ABSTRACT

This paper describes some of the basic principles and motivations underlying our brain-computer interface design. Our intent is to abstractly describe multi-rate filtering and orthogonal subspace decomposition appropriate for processing electroencephalographic data and identify some of the constraints imposed on the interface when considering a user with amyotrophic lateral sclerosis. Using an additive Gaussian noise model, orthogonal filter bank decomposition using a custom basis vector is demonstrated as an effective means for identification of events in an electroencephalogram.

INTRODUCTION

The University of Victoria Assistive Technology Team, (UVATT) is developing a non-invasive brain-computer interface, (BCI) to provide persons with a means to communicate when all other conventional methods have failed. More broadly, the technology under development may also be used to detect and characterize electrical parameters within the human brain associated with specific behavioural function. It is our hope that the signal processing approach discussed will improve assessment of conditions such as epilepsy, Huntington's disease, amyotrophic lateral sclerosis, (ALS, also known as motor neurone disease), and multiple sclerosis in the clinical environment by providing for improved quantitative measures.

Studies investigating neural disorders have been helpful in directing our BCI research and identifying candidate users and processing methods. Quantitative EEG, (QEEG) methods have suggested alpha band power, (7–12Hz) measured from the central scalp region (C3, C4, CZ, International 10-20 System electrodes) in persons with ALS decreases as the disease progresses [1] while other electrode sites do not exhibit this behavior. ALS has been of particular interest since this disease directly involves cortical motor neurons and therefore motivates development of a Brain-Computer Interface abstraction that does not necessarily rely on motor related EEG signals. Epilepsy is of interest as the impulse-like characteristics and theories relating to ionic sinks [2] provide clues to better understand the nature of EEG and how the EEG relates to the activity of neuronal functional units within the cortex. Eleptiform activity and non-stationary contributions to the EEG suggest signal processing methods that provide consideration for non-stationarity processes are better suited for this class of data than those methods that assume strong, wide-sense stationarity.

There are drawbacks to the use of scalp EEG to estimate user behaviour. Signal attenuation and low-pass filtering effects have created difficulties for measuring high frequency neural activity. Secondly, source localization has remained difficult as tissue impedances involved in the system are inconsistent in varied directions. One alternative to EEG, functional magnetic resonance imaging, (fMRI) measures haemodynamic response [3] to neural activity. Transient neural activity however can not be appropriately characterized by this method as fMRI requires integration times of approximately 1 second. Magnetoencephalography, (MEG) may be used as an alternative to EEG for examining high frequency brain activity however the financial barrier and physical size of the equipment make this technology inaccessible and unattractive for a BCI. Given these considerations, the scalp EEG is the most appropriate non-invasive interface to detect neural events.

In most clinical EEG settings, non-invasive techniques employ the International 10-20 Electrode System or a subset thereof. Typically, the signal-to-noise ratio obtained by the hardware is no greater than 90dB. The sampling rate for digital systems varies between 200 and 500 samples per second. Classically, EEG measured from the scalp is considered to have an upper frequency limit well below 100 Hz [4]. The signals examined in clinical analysis are generally between 10uV and 100uV as measured from a good scalp connection. Discrimination, identification, and signal processing parameters are commonly adjusted by the technician to make features of interest visible to the operator. When examining band-passed EEG, it is not always clear if one is examining a true narrow band oscillation or simply band-pass filtered white noise because noise power estimates are generally not used or not available.

Commonly a physiological response to a stimulus is used in conjunction with EEG to characterize neural activity within the brain. This evoked response testing employs ensemble averaging techniques to construct a clear picture of the electrical activity associated with the stimulus event. Ensemble averaging however assumes signal and noise stationarity [5] and a signal feature occurrence time-locked to the stimulus event. Variability in the response-time to a stimulus [4] and the contribution of non-Gaussian interfering processes reduce the potential quality of the result of evoked response testing using ensemble averaging trials as potential details are averaged out

of the result. Simply ensemble averaging EEG data therefore may not be the best means to extract weak features from EEG.

Techniques for estimating and removing muscle interference utilizing wavelet decomposition and independent component analysis have been proposed [6,7,8] and are currently being evaluated. Muscle activity measured by electromyography, (EMG) generally contains spectra as high as 2 kHz. When examining slow cortical potentials below 0.1 Hz, cable movements are a particular nuisance given the high gain of the EEG amplifiers as any cable movement or room vibration introduces artifacts. The usual method to reduce cable movement interference is set the lower cut-off frequency to some value above DC. A processing scheme addressing each of these noise sources without affecting detection of EEG features is highly desirable.

A demand for neural-controlled prosthetics, empirical assessment of motor control disabilities, and evaluation of human response to multi-media stimuli are attracting increasing interest and may come to drive the development of BCI technology. Industry [9,10] has already fostered corporate investment in technologies requiring implanted electrodes for their brain-computer interface design for humans.

A non-invasive but effective measurement system is of interest as the risks and costs associated with implant surgery are not always acceptable. Low data-rate, non-invasive BCIs have been developed by various researchers [11,12,13,14,15,16]. These groups have constructed multi-electrode scalp measurement devices utilizing standard EEG hardware that give the user simple control of a computer. In most cases, these devices rely on signals (evoked response, motor preparation peaks, alpha waves, and slow cortical potentials) that have been known to the clinical community for years. High data-rate, low error-rate, and cognitive control are our basic design parameters.

Our BCI design approach considers human neural physiology directly, utilizing fundamental centre theory models supporting compact neural representation of specific function, and characteristic tissue differences identified originally by Brodmann and further narrowed by functional imaging research. It is our hypothesis that these compact neural functions may be discerned in a signal-space characterized by ionic return paths mediated by glial cell arrangements. Glial cells outnumber neurons 10:1 and provide for the structure of these return paths [17].

Movement of a particular limb can generally be correlated with specific activity in motor areas however limitations to somatotopic organization exist as areas controlling a particular simple behaviour may overlap extensively with a different behaviour. When considering movement of thumb versus fingers in primates, somatotopic overlap and multiple limb representation exists in the primary motor cortex [18]. We extend this animal model to somatotopic organization in humans. Since our objective is not to specifically localize brain function but to discern characteristics from a signal-space perspective, we hope to differentiate between activation of neural networks in a common area and circumvent the problematic procedure of mapping signal sources to a canonical human brain. Surface electrode location and hemispheric dominance are still considered, however we view these as signal-to-noise parameters.

In developing a BCI we are interested in identifying a particular cognitive behaviour and not necessarily to differentiate between the physiological processes driving the behaviour. Thus, our task is to map features of the signal-space to a particular cognitive neuropsychological state. To facilitate an implementation that can detect feature events in real-time, allow for detection of features at multiple scales, provide good feature localization, and transform the data to better meet statistical assumptions, we have directed our attention to signal processing methods utilizing multi-rate filter bank decomposition and wavelet domain analysis.

The remainder of this paper is sectioned into the following parts. First, our early investigation and generation of signal models is provided for background. A description of the proposed EEG feature selection using blind deconvolution from which to derive a basis and the orthogonalization method to generate the basis is subsequently provided. Implementation of the orthogonalization of an arbitrary EEG component and filter bank noise removal is demonstrated. Finally, discussion of the signal processing methods and concluding remarks are provided. An illustration of the overall EEG feature selection methodology and real-time implementation of the feature detector is given in Figure 2.

NOMENCLATURE

Electroencephalography (EEG), Quantitative EEG (QEEG), Wavelet, Independent Component Analysis (ICA) , Blind Deconvolution, Brain-Computer Interface (BCI), Orthonormal Basis, University of Victoria Assistive Technology Team (UVATT), Slow Cortical Potential (SCP), Magneto encephalography (MEG), Functional magnetic resonance imaging (fMRI).

PRELIMINARY WORK

Self-initiated neural physiological function as well as function evoked by external sources bring about predictable changes in measured EEG. In past work, we have demonstrated subjects can cognitively modulate the EEG measured at their scalp [10]. In all cases examined in this preliminary study, persons with mid-term ALS were able to modulate the 7–12Hz band of their EEG from the PZ electrode. Figure 1 illustrates the modulated EEG of one of the subjects. The model used to justify this detector is given as $q(t) = x(t) + w(t)$, where $w(t)$ is the white noise component and $x(t)$ is a single frequency represented as $\cos(wt + j)$ with a random frequency, phase, and probability of occurrence.

We've since generalized our model so that it can be applied to a wider range of EEG components and can account for non-Gaussian interferers. The models to be considered in current and future work are defined as

$$q(t) = x(t) + w(t) + n(t) \text{ and} \qquad (1)$$

$$q(t) = \sum \hbar_n \{x(t), r_i(t)\} + w(t) + n(t) + m(t) \qquad (2)$$

where $w(t)$ is the white noise component visible at all frequencies including those greater than the highest non-Gaussian process in a sampled EEG spectrum, $n(t)$ represents proximal cortical interferers modeled as additive non-Gaussian interference, $m(t)$ includes muscle noise contributions, $x(t)$ is the feature of interest, $r_i(t)$ and $\hbar_n\{.\}$ model nonlinear thalamic excitation and inhibition of cortical areas [16]. Each interfering component has some random probability of occurrence.

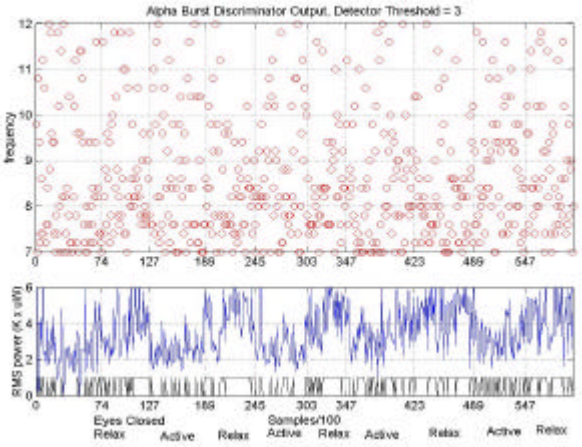

Figure 1: The plotted results of simple alpha-band power measurements from the PZ electrode of a person with mid-term ALS. RMS power and frequency was measured using a sliding 1 second Hanning window cosine matched filter arrangement. Data were collected at 200 samples per second. Subjects were asked to close their eyes and then relax and visualize clouds, or actively solve mathematical problems without feedback. The figure illustrates a test of approximately 5 minutes with 4 active segments and 5 relaxed segments.

Since an EEG record, $q(t)$ is not necessarily stationary over an analysis window that includes both short duration and long duration events, multi-resolution analysis is more appropriate than Fourier analysis using a fixed window size. If only a single analysis window is used, and both long-duration and short-duration processes are of interest, the minimum window size is constrained to include the longest duration feature of interest. By using a large window to accommodate the long-duration feature, the statistical contributions of the short-duration features may be de-emphasized. Multi-resolution analysis implemented using filter bank decomposition provides an efficient method to process features of varied duration and provide for good time localization of these features. Additionally, the basis used in the multi-resolution filter bank analysis need not be a Fourier basis. A basis more suitable for detection of features in EEG may be selected for the decomposition, and may be derived from the EEG itself.

FEATURE SELECTION

Candidate basis functions for a real-time detector may be identified by applying blind deconvolution to EEG collected under controlled conditions. Blind deconvolution employing ICA exploits the property that component independence implies these components are also uncorrelated. Independence also implies a possibility of factorization by nonlinear correlation [19], as is demonstrated by Equation 3 and Equation 4.

Given the nonlinear transformations and combination of two random vectors $\mathbf{x}$ and $\mathbf{y}$, the expected value may be written as Equation 3 where $p(\mathbf{x},\mathbf{y})$ is the joint probability function.

$$? [\mathbf{g}_1(\mathbf{x})\mathbf{g}_2(\mathbf{y})] = \int\int \mathbf{g}_1(\mathbf{x})\mathbf{g}_2(\mathbf{y})\, p(\mathbf{x},\mathbf{y})\, d\mathbf{x}d\mathbf{y} \qquad (3)$$

If the joint probability can be factored as $p(\mathbf{x},\mathbf{y}) = p(\mathbf{x})p(\mathbf{y})$, then $\mathbf{x}$ and $\mathbf{y}$ are statistically independent [5]. Given statistical independence and the nonlinear transforms $\mathbf{g}_1(\mathbf{x})$ and $\mathbf{g}_2(\mathbf{y})$ we can factor the nonlinear correlation $\mathrm{E}[\mathbf{g}_1(\mathbf{x})\mathbf{g}_2(\mathbf{y})]$ as in Equation 4.

$$\mathrm{E}[\mathbf{g}_1(\mathbf{x})\mathbf{g}_2(\mathbf{y})] = \int \mathbf{g}_1(\mathbf{x})\, p(\mathbf{x})\, d\mathbf{x} \int \mathbf{g}_2(\mathbf{y})\, p(\mathbf{y})\, d\mathbf{y} = \mathrm{E}[\mathbf{g}_1(\mathbf{x})]\mathrm{E}[\mathbf{g}_2(\mathbf{y})] \qquad (4)$$

Using the ICA format, $\mathbf{z} = \mathbf{A}\mathbf{s}$, independence of the source components $\mathbf{s}$ is therefore sufficient to solve for the inverse of $\mathbf{A}$. Since independence infers factorization of the nonlinear correlation and the data contains high order statistical properties, statistics beyond 2nd order may be used to separate signal components [19,20]. The nonlinear operation through which the high order statistical properties are generated should be tailored to the data in question [19].

The degree to which results obtained from blind deconvolution are compatible with an orthonormal filter bank decomposition will be the focus of future work. A description of orthogonal filter bank decomposition and theory in terms of differentiating between generators from a signal-space and function-space perspective follows.

SIGNAL-SPACE DECOMPOSITION

Given that W_{j+1} and V_{j+1} are orthogonal components of V_j in Equation 5, where V_{j+1} is the scaling or aggregate space, and W_{j+1} is the detail space, the detail space may be viewed as the difference between V_j and V_{j+1} where $\oplus$ indicates an orthogonal relation. Equation 5 and Equation 6 demonstrate the recursive relationship between spaces.

$$V_j = V_{j+1} \oplus W_{j+1} \qquad (5)$$

$$V_j = W_{j+1} \oplus W_{j+2} \oplus W_{j+3} \oplus V_{j+3} \qquad (6)$$

Between each subspace decomposition, V_j into V_{j+1} and W_{j+1}, the input vector is decimated by 2 providing for orthogonality of scale. Scale increases with j while time increases with t and shifts with k. A particular subspace is denoted by its j-k coordinate. In terms of function spaces, function *f(t)* contained in V_{j+1} is *f(2t)* in the subspace V_j. If a function *f(t)* is in V_{j+1}, then all it's translates *f(t-k)* and translations of it's dilations *f(2t-k)* are in V_j. This property is known as shift invariance and provides for orthogonality between translates. Extending the function $f(t)$ to an arbitrary basis function for a given scale j and translation k, the relationship is as $f_{jk}(t) = j_{jk}(t) = 2^{j/2} j(2^j t - k)$, where $j(2^j t - k)$ is the normalized arbitrary basis function and $2^{j/2}$ is a scaling factor between scales *j* for a dyadic decomposition. A function decomposition and the corresponding expansion at a particular scale is given as Equation 7. A complete expansion is demonstrated as Equation 8.

$$f_j(t) = \sum_{-\infty}^{\infty} a_{jk} j_{jk}(t) \tag{7}$$

$$f_{jk}(t) = \sum_k a_{0k} j(t-k) + \sum_k b_{0k} W(t-k) + \sum_k b_{1k} 2^{1/2} W(2t-k) + \ldots \tag{8}$$

Given the properties of shift invariance and dyadic decomposition, each space is orthogonal to the next in both time and scale. The wavelet domain resultant represents each time and scale as a discrete quantity of energy.

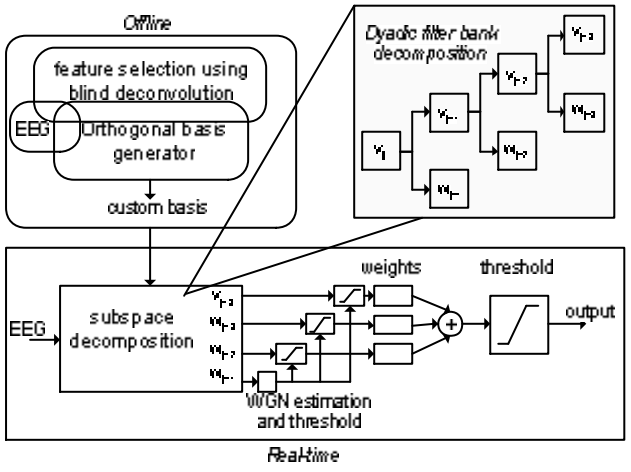

Figure 2: Block diagram illustrating off-line feature selection using blind deconvolution and orthogonal basis generation to create a custom basis, and the relation to real-time feature detection using subspace decomposition.

GENERATING A CUSTOM BASIS

A custom basis vector was generated using the Broyden – Fletcher – Goldfarb – Shanno, (BFGS) [21] minimization algorithm combined with a polyphase matrix to generate basis coefficients. This was used instead of Gramm-Schmidt orthogonalization as the polyphase representation generates double-shift orthogonal FIR coefficients suitable for a dyadic decomposition filter bank [22]. The orthonormal basis generation is illustrated in Figure 3 and related to the overall system in Figure 2 All calculations and plots were done using MATLAB.

A cascade of rotation and delay matrices was used to constrain the optimization to generate an orthonormal structure. The filter bank cascade algorithm [22] was then used to generate the coefficients corresponding to a particular filter bank decomposition level. Each matrix in the cascade was restricted to orthogonality by the arrangement of functions within the each rotation matrix. The cascade of orthogonal matrices was restricted to orthogonality [22] by constraining the rotation angles, $f_0, f_1, \ldots, f_\ell$ in the cascade to sum to $p/4$.

Using notation from [22], the polyphase matrix for the complete lattice arrangement is given as Equation 9 and Equation 10. The function $\Lambda(z)$ is a diagonal delay matrix. The factor $\Lambda(-1)$ was included to mu ltiply the components of the odd phase of the high-pass filter by (-1). Components $R_\ell .. R_0$ represent rotation matrices. A single rotation with one delay is noted as $H_p^\ell(z) = R_\ell \Lambda(z)$ where ℓ is a rotation angle index for the cascade of rotation matrices. Equation 11 and Equation 12 demonstrate the relationship between the FIR filter coefficient vectors, ***c*** and ***d***, and the polyphase matrix.

$$H_P(z) = \Lambda(-1) R_\ell \Lambda(z) R_{(\ell-1)} \ldots R_1 \Lambda(z) R_0 \tag{9}$$

$$H_P(z) = \Lambda(-1) \begin{bmatrix} \cos(f_\ell) & \sin(f_\ell) \\ -\sin(f_\ell) & \cos(f_\ell) \end{bmatrix} \begin{bmatrix} 1 & 0 \\ 0 & z^{-1} \end{bmatrix} H_p^{\ell-1} \ldots H_p^1 H_p^0 \tag{10}$$

A recursive algorithm was created to generate the polyphase matrix and extract FIR coefficients for use with the filter bank cascade algorithm. The FIR coefficients were extracted from odd and even components of the polyphase matrix.

$$H_P(z) = \begin{bmatrix} c_0 + c_2 z^{-1} + c_4 z^{-2} & c_1 + c_3 z^{-1} + c_5 z^{-2} \\ d_0 + d_2 z^{-1} + d_4 z^{-2} & d_1 + d_3 z^{-1} + d_5 z^{-2} \end{bmatrix} \tag{11}$$

$$H_P(z) = \begin{bmatrix} c_{even} & c_{odd} \\ d_{even} & d_{odd} \end{bmatrix} \tag{12}$$

Since the resulting objective function for minimization contained numerous local minima, random starting points were used to search for a global minimum. To generate 30 FIR coefficients, the minimization problem utilized 14 rotations and 1 scaling variable.

Some constraints on the EEG feature to which we matched a basis vector were necessary because the orthogonality constraint and the small number of rotation angles heavily limited possible approximation accuracy. Care was taken in selecting a feature to be as sparse in details as reasonable

minimization would allow. Additionally, since the basis vector is required to have zero mean, values that approach zero at the window edges, and a band-limited spectrum, the EEG feature vector selected for approximation was restricted to have the same properties.

In short-form, the objective function minimized is given as Equation 13,

$$F = E\{T\{f(R([f_1, f_2, ..., f_{13}, f_{14}, A^2]))\}\} \quad (13)$$

where *R(.)* is the rotation matrix operation, *f(.)* denotes the angle to FIR coefficient conversion, *T(.)* corresponds to the cascade algorithm, and *E(.)* is the difference between the approximation and the actual EEG feature as measured using the L-2 norm. Scaling of the EEG feature vector by A^2 was required to have the minimization function approach zero since we did not directly restrict the EEG feature vector for approximation to have unit norm. Since the BFGS algorithm itself does not constrain A to only positive values, the scale factor was squared to prevent the algorithm from reversing the sign during the minimization process.

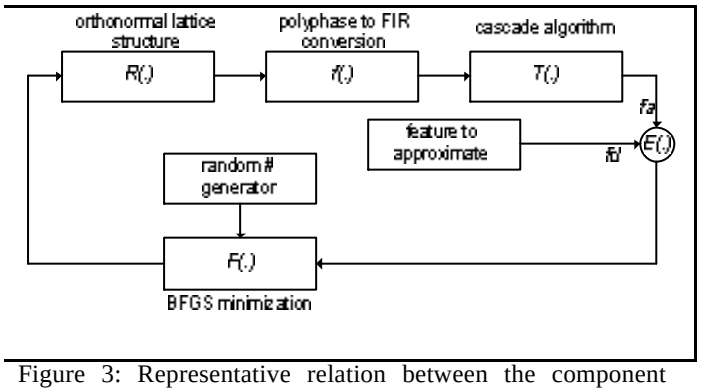

Figure 3: Representative relation between the component algorithms necessary for the orthonormal optimization problem.

The error function of Equation 14 measures the least squares difference between the current approximation, ***fa*** and the EEG feature to approximate, ***fd***.

$$E = \sum_{i=0}^{N-1} \| fd[i] - fa[i] \|_2^2 \quad (14)$$

The constraint that the sum of rotation angles must add to $p/4$ for an orthogonal filter bank was made implicit to the unconstrained minimization algorithm by reducing fifteen rotation angles, j_0 to j_{14} to fourteen rotation angles. Angle, j_0 was equated to the other fourteen angles as illustrated in Equation 15. The overall transform and optimization process is illustrated in Figure 3.

$$j_0 = (p/4) - (j_1 + j_2 + j_3 + j_4 + ... + j_{14}). \quad (15)$$

DETECTION AND NOISE ESTIMATION

For demonstration purposes, level-5 detail coefficients of a dyadic filter bank were optimized to a selected EEG feature. The wavelet-domain impulse response of the reconstruction filter is illustrated in Figure 4 For the actual implementation, feature detection will take place using wavelet domain coefficients as illustrated in Figure 2.

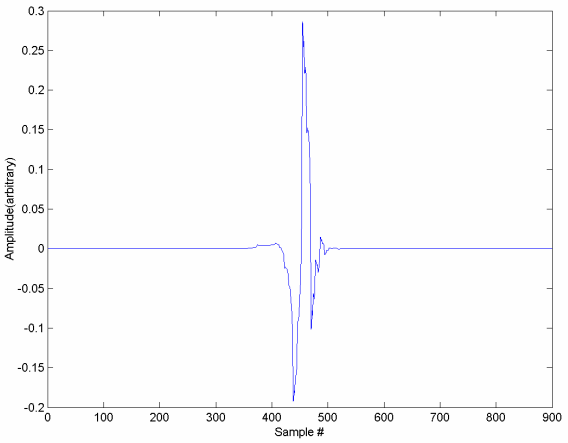

Figure 4: The detail level-5 wavelet-domain impulse response of the reconstruction filter with no additive noise.

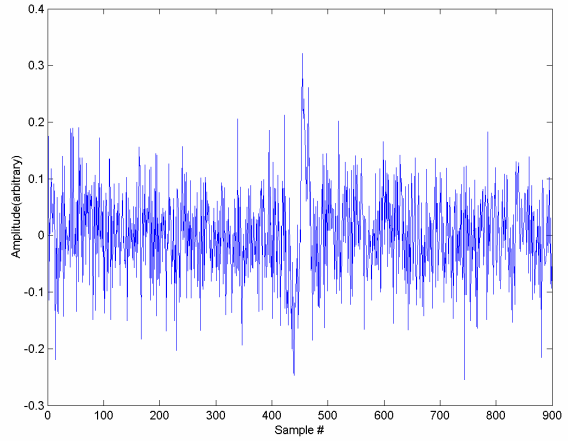

Figure 5: Feature with Gaussian interference to be extracted by the filter bank and custom basis.

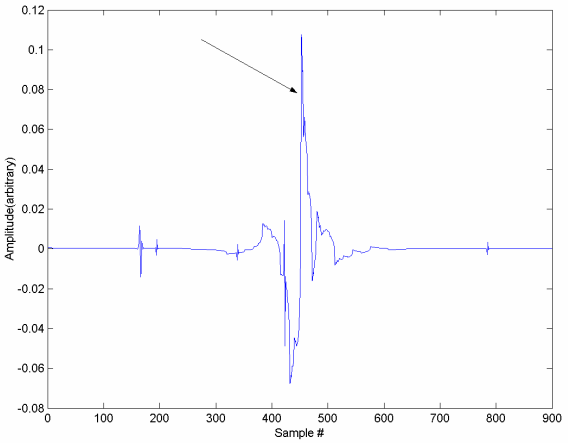

Figure 6: Recovered feature using the described denoising method and custom basis.

A procedure proposed by Donoho [23], for estimating the power of the white Gaussian noise component of a signal and subtracting this estimated component was examined to demonstrate feature extraction from an EEG. Donoho's proposed methodology utilizes the highest detail level of a dyadic wavelet decomposition to estimate the power of an interfering white Gaussian noise process, assuming that there is no energy from other processes at this scale. Once the noise power is estimated using the highest detail level wavelet coefficients, the wavelet coefficients at all scales are thresholded by a function of the estimated noise power. Once the coefficients have been thresholded appropriately, the time-domain signal may be re-constituted using a reconstruction filter bank. Since this method requires that there is no energy other than that of the white Gaussian noise process at the highest detail level of the wavelet decomposition, a sampling frequency greater than four times the highest frequency of all non-white processes is required. Ultimately, this method provides a mechanism to determine if the output of a detector is a result of the feature of interest or a result of background white noise.

To demonstrate the effectiveness of this noise estimation method, Donoho's methodology was used to de-noise a feature of unit energy buried in white Gaussian noise of variance equal to 0.0059. The filter bank and basis vector used to de-noise and re-constitute the non-white process was derived using the optimization method described previously. The example feature was derived from the detail level-5 wavelet domain impulse response. The basis vector used to implement the filter bank is an approximation derived of an arbitrary EEG feature using the orthogonalization algorithm described previously. Figure 4, Figure 5, and Figure 6 are provided to qualitatively illustrate the effectiveness of the de-noising process. The Soft Shrinkage method [23] was used to threshold the wavelet coefficients based on the estimate of the power of the noise process at the highest detail level of the filter bank decomposition.

DISCUSSION

The filter bank orthogonal decomposition is not limited to the dyadic decomposition demonstrated. The branching structure may be determined by such measures as maximum entropy [22] to reduce the energy at any given node to a predetermined minimum. This strategy serves to further maximize the difference between a selected feature for detection and non-white interfering processes.

In constructing our basis vector, we optimized only for detail level-5 of the filter bank. It is necessary to further examine the role convergence of the cascade algorithm plays on estimation of the feature of interest in non-optimized detail levels. It may also prove to be more efficient to first optimize levels with a small number of coefficients by down-sampling the EEG feature to approximate and then subsequently optimize higher detail levels.

The key reason for using filter bank decomposition of an EEG for feature detection is to provide multiple window sizes to better meet the stationarity requirements of statistical processing. A detector may further evaluate the statistics of the EEG by examining the wavelet domain coefficients at each decomposition level.

There are strict properties that the selected EEG feature must adhere to for the objective function minimization result to potentially qualify as a wavelet. We hope to address this in future work by using blind deconvolution to search for statistically independent EEG components that also support the properties of an orthonormal wavelet. This may not be completely successful however the results should point to an appropriate wavelet upon which a maximum entropy decomposition tree can be selected instead of arbitrarily selecting a class of Daubechies wavelet and dyadic decomposition.

CONCLUSIONS

The visual effectiveness of the filter bank de-noising and reconstruction of the detected feature is apparent from Figure 6. If we further limited reconstruction of coefficients to the detail-5 level, artifacts in other scales would be completely removed. One might take this step if apriori knowledge of scale of the feature to be detected was available.

One major drawback to the optimization method described in this paper is the calculation time required for our implementation of the polyphase matrix to FIR coefficient conversion. The optimization process currently takes on the order of days for 80 starting points, 15 optimization variables at a level-5 cascade. The time required could be reduced by constructing a lattice implementation of the filter bank instead of converting the lattice angle solutions to FIR coefficients during each iteration of the minimization algorithm. Additionally, a lattice implementation would eliminate errors associated with rounding [22].

For the estimation of the power in the white Gaussian noise component of an EEG, and to appropriately include muscle interference, it is necessary to construct acquisition hardware with appropriate dynamic range and sampling frequency. We are currently constructing an 8 channel, 24-bit USB EEG acquisition system that should have a CMR of approximately 100 dB.

Future work will evaluate the suitability of blind deconvolution to identify a wavelet upon which a filter bank can be constructed or used subsequent to a Debauches wavelet decomposition. Furthermore, we will investigate whether or not independent signal component identification implemented using filter banks will truly enable us to differentiate between the activity of proximal neuronal functional units within the cortex and underlying midbrain activity as measured from scalp EEG.

To aid in the evaluation of detection techniques, we will further examine how macroscopic neuronal circuits and corresponding ion feedback paths with the filtering effects of the scalp may be modeled as a transfer function with specific inputs and outputs. Future work will use these models to run simulations to determine error rates associated with a variety of detection schemes.

Aside from the research and medical applications afforded, following UVATT's mandate, the efforts discussed in this paper will be used to construct a non-invasive, portable, BCI that will be available to meet the needs of disabled persons within our community.

ACKNOWLEDGMENTS

We would like thank Vivian Sin, the staff in the Biomedical Department of Vancouver General Hospital, Vancouver, BC, Canada. Other thanks to Sharon Livingstone, Ron Skelton, Michael Young, and the late Claire Minkley, for their support and inspiration. UVATT is a non-profit organization, created as a community resource for the development of assistive devices.

Permission for human studies was granted University of Victoria, BC, Canada.

REFERENCES

[1] R. Mai, D. Facchetti, A. Micheli, M. Poloni, "Quantitative electroencephalography in amyotrophic lateral sclerosis," *Elecroencephalography and Clincal Neurophysiology*, vol. 106, no. 4, pp. 383-386. 1998.

[2] Marco de Curtis, G. Avanzini, "Interictal spikes in focal epileptogenesis," *Progress in Neurobiology*, vol. 63, pp. 541-567. 2001.

[3] N. K. Logothetis, "The neural basis of the blood-oxygen-level-dependent functional magnetic resonance imaging signal," *Philos. Trans R. Soc. Lond. B. Biol. Sci.*, vol. 357, 1003-10037. August 2002.

[4] N. Burch, H. L. Altshuler. *Behavior and Brain Electrical Activity*. New York: Plenum Press. 1975.

[5] P. Z. Peebles, JR, *Probability, Random Variables, and Random Signal Principles*. New York: McGraw-Hill. 1993.

[6] R. Vigário, V. Jousmäki, M. Hämäläinen, R. Hari, and E. Oja, "Independent component analysis for identification of artifacts in magnetoencephalographic recordings," in *Advances in Neural Information Processing Systems*, vol. 10, pp. 229-235. 1998.

[7] Tzyy-Ping Jung, Scott Makeig, Colin Humphries, Te-Won Lee, Martin J. Mckeown, Vicente Iragui, Terrence J. Sejnowski, "Removing Electroencephalographic Artifacts by Blind Source Separation," *Psychology*, vol. 37, pp. 163-178, Cambridge University Press. 2000.

[8] Tatjana Zikov, Stephane Bibian, Guy A. Dumont, Mihai Huzmezan, "A Wavelet Based De-Noising Technique for Ocular Artifact Correction of the Electroencephalogram," Department of Electrical and Computer Engineering, University of British Columbia, BC, Canada. 2002.

[9] Cyberkinetics Inc., Foxborough, MA, USA.

[10] Neural Signals Inc., Atlanta, GA , USA.

[11] W. Hook et al., "Brainwave Communication, Coherent Detection Processing and Results," University of Victoria, Victoria, BC, Canada, Seminar. 2002.

[12] W. D. Penny and S. J. Roberts, "Experiments with an EEG-based computer interface," Department of Electrical Engineering, Imperial College, London, England. 1999.

[13] Wolpaw, McFarland, Neat, Forneris, "An EEG-based brain-computer interface for cursor control," *Electroencephalography and Clinical Neurophysiology*, vol. 78, pp. 252-259. 1991.

[14] G. Pfurtscheller, C. Neuper, A. Schloegel, K. Lugger, "Separability of EEG signals recorded during right and left motor imagery using adaptive autoregressive parameters," *IEEE Transactions on Rehabilitation Engineering*, vol. 6, no. 3, pp. 316-325. 1998.

[15] J.R. Wolpaw, D.J. McFarland, "Multichannel EEG-based brain-computer communication," *Electroencephalography and clinical Neurophysiology*, vol. 90, pp. 444-449. 1994.

[16] G. E. Birch, Z. Bozorgzadeh, S. G. Mason, "Initial On-Line Evaluations of the LF-ASD Brain-Computer Interface with Able-Bodied and Spinal-Cord Subjects using Imagined Voluntary Motor Potentials," *IEEE Trans. Neural Sys. And Rehab. Engineering*, vol. 10, no. 4, pp. 219-224. December 2002.

[17] E. R. Kandel, J. H. Schwartz, T. M. Jessell, *Principles of Neural Science*. New York: McGraw-Hill, Health Professions Division. 2000

[18] M. H. Schieber, "Constraints on Somatotopic Organization in the Primary Motor Cortex," Departments of Neurology, Neurobiology and Anatomy, Brain and Cognitive Science, and Physical Medicine and Rehabilitation, the Center for Visual Science, and the Brain Injury Rehabilitation Program at St. Mary's Hospital, University of Rochester School of Medicine and Dentistry, Rochester, New York. 2001.

[19] Tadeusz Ulrych, Sam Kaplan, "Blind Deconvolution via Independent Component Analysis," Department of Earth and Ocean Sciences, University of British Columbia, BC, Canada. 2002.

[20] A. Hyvarinen, J. Karhunen, E. Oja, *Independent Component Analysis*. New York: John Wiley & Sons. 2001.

[21] D. G. Luenberger, Linear and Nonlinear Programming, 2nd ed., Reading, MA: Addison-Wesley. 1984.

[22] G. Strang, T. Nguyen, *Wavelets and Filter Banks*. Wellesley-Cambridge Press. 1996.

[23] D. L. Donoho, "De-noising by Soft-Thresholding," Department of Statistics, Stanford University, USA. 1992.